Title	High frame rate vector flow imaging of stenotic carotid bifurcation: computational modeling and analysis
Author(s)	Chan, DLS; Yiu, BYS; Yu, ACH
Citation	The 2011 IEEE International Ultrasonics Symposium (IUS), Orlando, FL., 18-21 October 2011. In IEEE International Ultrasonics Symposium Proceedings, 2011, p. 409-412
Issued Date	2011
URL	http://hdl.handle.net/10722/140229
Rights	IEEE International Ultrasonics Symposium Proceedings. Copyright © IEEE.

10.1109/ULTSYM.2011.0098

High Frame Rate Vector Flow Imaging of Stenotic Carotid Bifurcation: Computational Modeling and Analysis

Donald L. S. Chan, Billy Y. S. Yiu and Alfred C. H. Yu

Medical Engineering Program,
The University of Hong Kong, Pokfulam, Hong Kong SAR

Corresponding Email: alfred.yu@hku.hk

***Abstract*—Analysis of the complex blood flow pattern in the carotid bifurcation is clinically important to the diagnosis of carotid stenoses. We hypothesize that the use of high frame rate imaging methods such as plane wave excitation, together with vector flow estimators like block matching, may potentially be a suitable imaging problem to this problem. This paper presents our team's initial efforts in developing a high frame rate vector flow imaging framework that is based on plane wave excitation principles and a high dynamic range block matching algorithm that incorporates least squares fitting principles. We have conducted a series of Field II simulations on straight tubes and carotid bifurcation to evaluate the estimation accuracy and imaging performance of our framework. Results indicate that high-frame-rate vector flow imaging is capable of visualizing complex blood flow. It has potential to be further developed into a new clinical technique for vascular diagnoses.**

***Index Terms*—stenotic carotid bifurcation, high frame rate, vector flow imaging, CFD modeling**

I. Introduction

Stroke refers to the loss of brain functioning due to blockage of blood supply to the brain [1], and patients may suffer from inability to see, control limbs, or formulate speech. It is well-accepted that one of the major stroke symptoms is carotid artery stenosis: the narrowing of carotid artery lumen as a result of deposition of fatty substances. Various clinical studies have suggested that proper early intervention of carotid artery stenosis can significantly reduce the risk of stoke [2], [3]. As such, development of effective and reliable carotid artery stenosis screening tools has long been of great medical interest.

As a non-invasive beside imaging modality, ultrasound color flow imaging (CFI) is often considered as an image-based carotid stenosis screening tool that can be used in conjunction with spectrogram-based Doppler ultrasound measurements. Clinicans would make use of CFI together with Doppler ultrasound to classify patients into categories (mild, moderate and severe) based on the thickness of the deposition and peak systolic velocity of internal carotid artery [3]. Nevertheless, on its own, CFI is not recommended for use as a screening tool for carotid stenosis because of a few technical reasons that demerit its diagnostic accuracy [4]. First, CFI can only provide axial flow estimates that are in parallel to the ultrasound beam direction, and this inherently results in biased flow visualization in cases where the beam-flow angle varies over the imaging view. Second, the frame rate of CFI may not be sufficient to provide an accurate mapping of the actual flow conditions, because its imaging scheme is based upon a beamline-based multi-firing sequence that inherently requires a significantly longer data acqusition time than B-mode imaging.

In recent years, efforts have been devoted to the development of high-frame-rate vector flow imaging (VFI) methods that can overcome the technical limitations of CFI. This framework is in principle capable of achieving imaging frame rates of greater than 1000 fps (through the use of fast data acquisition methods like plane wave excitation), as well as providing directional flow estimates independent of the beam-flow angle. As such, we hypothesize that this emerging modality has potential in establishing itself as a more capable image-based screening tool for carotid stenosis as compared to CFI. In this paper, we present a feasbility study on applying high-frame-rate VFI to carotid stenoses. We shall present our technical innovations in developing a high dynamic range (HDR) block matching algorithm for accurate vector flow estimation when using high-frame-rate data acquisition techniques. We will also discuss its performance in visualizing complex flow profiles generated from a computational model on stenotic carotid bifurcation.

II. Theory

A. High-Frame-Rate Data Acquisition

To achieve high imaging frame rate, we have made use of the plane wave excitation data acquistion algorithm. This technique works by exciting all elements of the ultrasound transducer at the same time to generate a broad wavefront covering the whole image region on transmission [5]. All array channels are then used to collect pre-beamformed data in parallel, after which parallel beamforming of multiple image lines is performed from the acquired channel-domain data.

In contrast to conventional scanline-based data acquisition algorithm, a frame instead of a scanline can be obtained for each firing. In other words, the achievable frame rate is the same as pulse repetition frequency (PRF) that is usually greater than 1000fps. It ensures that the imaging frame rate is sufficient to resolve the flow patterns in various cardiac cycle phases.

B. High Dynamic Range (HDR) Block Matching Algorithm

In carotid artery stenosis diagnoses, the blood flow pattern is rather complex both spatially and temporally, with velocity ranging from several cm/s up to several m/s [2]. Therefore the dynamic range is a crucial factor determining the detection accuracy of carotid artery stenosis. In general, the dynamic range of block matching is governed by the size of search region. Nonetheless, when a larger search region is used, the probability of peak hopping increases and this may affect the estimation accuracy [6]. To account for this issue, we have developed a HDR block matching algorithm that is based on temporal averaging of velocity estimates.

An overview of our developed algorithm is illustrated in Fig. 1. The algorithm begins with the formation of an ensemble matrix by stacking up n B-mode images. For the estimation of each pixel, a kernel (with dimension $l \times k$) centered around the pixel position is identified in the first frame of the image ensemble, and a corresponding search region is delineated in the $n-1$ subsequent frames in the ensemble. Block matching is then applied between the first frame and each of the $n-1$ subsequent frames, and the sum of absolute difference is used as the matching criteria to identify the coordinates (α_i, β_i) that minimize the following cost functionε:

$$\varepsilon(\alpha_i, \beta_i) = \sum_{x=1}^{l} \sum_{z=1}^{k} |\mathbf{K}(x,z) - \mathbf{S}_i(x+\alpha_i, z+\beta i)|, \qquad (1)$$

where $\mathbf{K}$ is the kernel and $\mathbf{S}_i$ is the i^{th} search region in the image ensemble. Once the block matching process is completed for all $n-1$ frames in the ensemble, a least squares fitting procedure is applied individually to the set of raw axial estimates α_i and lateral estimates β_i to compute the average velocity vector estimate over the n-frame ensemble. In particular, our goal is to find the velocity component in each of the following two equations:

$$\begin{matrix} \alpha_i = v_x t_i + c_1 \\ \beta_i = v_z t_i + c_2 \end{matrix}, \qquad (2)$$

where v_x and v_z are lateral and axial velocity, t is the time of reference and c_1 and c_2 are constants. Since there are $n-1$ displacement estimates for each pixel in each ensemble, we can solve the above equation by grouping the displacement estimates together to form the following system of equations (axial estimate shown as example):

$$\begin{bmatrix} \alpha_1 \\ \alpha_2 \\ \vdots \\ \alpha_{n-1} \end{bmatrix} = \begin{bmatrix} t_1 & 1 \\ t_2 & 1 \\ \vdots & \vdots \\ t_{n-1} & 1 \end{bmatrix} \begin{bmatrix} v_x \\ c_1 \end{bmatrix} \Rightarrow \mathbf{A} = \mathbf{T}\mathbf{v}, \qquad (3)$$

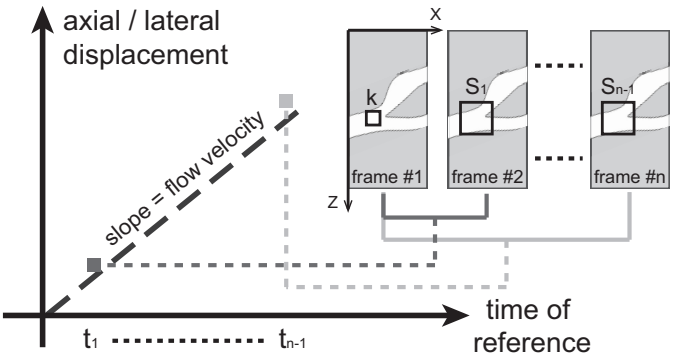

Fig. 1. Illustration of the HDR block matching algorithm. Successive displacement estimates were obtained by matching the kernel ($\mathbf{K}$) over search regions ($\mathbf{S}_1$, $\mathbf{S}_2$ ...$\mathbf{S}_{n-1}$) obtained at different time point. Least square fitting is applied to the axial and lateral displacement estimates independently for flow velocity measurement.

The least squares estimation of $\mathbf{v}$ can be calculated by multiplying the pseudoinverse of $\mathbf{T}$ with $\mathbf{A}$:

$$\mathbf{v} = \mathbf{T}^{\dagger}\mathbf{A}, \qquad (4)$$

where the † superscript refers to the pseudoinverse operation. Note that a similar operation can be performed to the lateral displacement estimates β_i to estimate the lateral velocity.

III. Initial Analysis: Straight Flow Tube Model

A. Simulation Procedure

To evaluate the estimation accuracy of the proposed high frame rate VFI framework, two series of straight flow tube phantom simulations have been performed: 1) fixed beam-flow angle of 60° with flow velocity ranging from 10 - 50 cm/s, and 2) fixed flow velocity of 25 cm/s with beam-flow angle ranging from 15° - 75°. The diameter of the flow tube is 6 mm, and a parabolic flow profile has been adopted. For each flow scenario, 30 sets of pre-beamformed data were generated using Field II [7], [8] (center frequency: 5 MHz; transmit pulse duration: 2 cycles; pulse repetition frequency: 5 kHz; slow-time ensemble size: 12). The acquired data were beamformed to form B-mode images using the delay-and-sum algorithm and dynamic receive focusing principles. A first-order polynomial regression filter was applied to remove clutter prior to the velocity estimation. In this work, kernel and search region were selected as a square window with dimensions of $1 \times 1\, mm^2$ and $2 \times 2\, mm^2$ respectively.

B. Results: Estimation Accuracy

Fig. 2 shows the estimation performance of the framework. In general, it can be seen that the velocity and angle estimates are close to the actual values. Our quantitative analysis indicates that the average estimation biases are 1.61 cm/s and 3.23 cm/s respectively for the axial (Fig. 2a) and lateral velocity estimates (Fig. 2b). The small range of standard deviation for the velocity estimates (indicated by the error bars) also demonstrate the estimation consistency of our algorithm. It should be noted that when the beam-flow angle is greater than

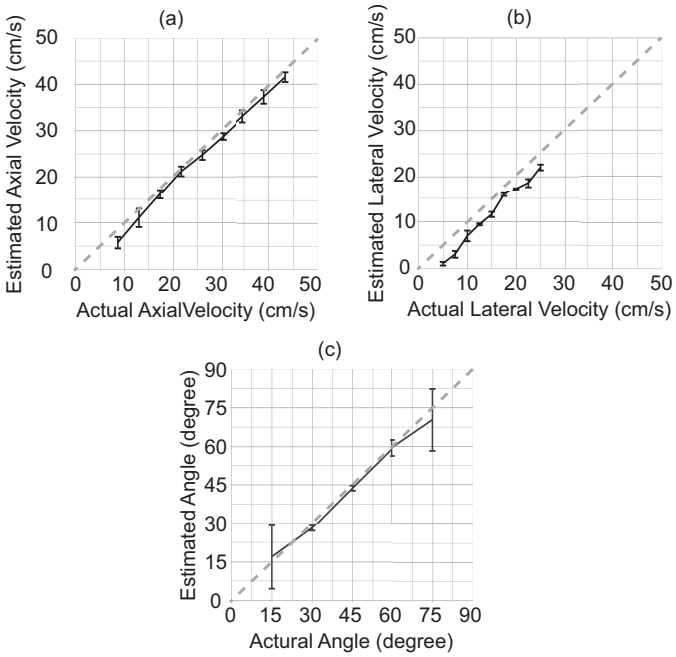

Fig. 2. Estimation performance of (a) axial velocity, (b) lateral velocity and (c) beam-flow angle estimation (error bars indicate standard deviation). The dotted lines indicate the ideal case with no estimation error. (a) and (b) are obtained with fixed beam-flow angle of 60°, so the effective range of axial velocities (8.7-43.3 cm/s) is expectedly larger than that for lateral velocities (5-25 cm/s). (c) is obtained with fixed flow velocity at 25cm/s.

75° or less than 15°, a significantly higher variance in angle estimation can be seen. This issue will be further discussed towards the end of this paper.

IV. Further Analysis: Carotid Bifurcation Model

A. Computational Modeling

To examine the applicability of high-frame-rate VFI in carotid artery stenosis diagnoses, a more realistic carotid bifurcation phantom simulation study was carried out. The phantom geometry was based upon the eccentric stenosed model proposed by Smith et al. [9]. Three models representing normal (0%), moderate (40%) and severe stenosed (80%) bifurcation were considered, and computational fluid dynamic (CFD) simulations were conducted to calculate complex blood flow within these models using the Fluent software (ver 6.3.26; ANSYS). The inlet boundary was set to be a pulsatile flow profile and both outlets were set to be the human mean arterial blood pressure (100 mmHg). Blood was assumed to be an incompressible Newtonian fluid with dynamic viscosity and density of 3.5 mPa·s and 1050kg/m^3 respectively. The calculated blood flow patterns were then imported to MATLAB as scatterer displacement input for Field II simulations (imaging parameters were the same as the straight-tube study).

B. Analysis Procedure

Both CFIs and VFIs were generated for the bifurcation phantom to facilitate comparative assessment. The CFIs were obtained using scanline-based data acquisition algorithm with

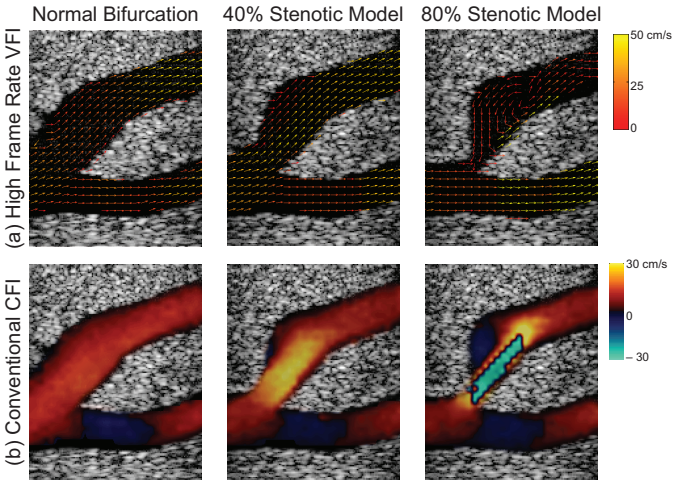

Fig. 4. Flow visualization results for (a) high frame rate VFI and (b) Conventional CFI. The arrow color of each range gate in (a) represents the flow magnitude whereas the arrow indicates the flow direction.

transmit focus at 30 mm depth. The aperture size was set as 32 elements and result in 97 scanlines over the field of view. Clutter filtering was performed using a first order polynomial regression filter, and lag-one autocorrelator was used for flow velocity estimation. For the VFIs, they were computed according to the algorithms mentioned in Section II. Flow direction and velocity magnitude were depicted as arrows and hot colormap hues respectively.

C. Results: Imaging Performance

The analysis results generally show that high frame rate VFI can provide more accurate diagnosis information comparing with conventional CFI. Fig. 3 (plotted on next page) shows the flow images of severe stenosed bifurcation model obtained during the peak systole phase (time interval = 0.1s). During this period, 40 high frame rate vector flow images can be obtained. Such a frame rate enables visualization of the blood flow pattern during peak systole phase. In contrast, conventional CFI can only provide flow information in less than half a frame. Even if sufficient time is provided for the acquisition of a whole CFI, the flow information of that image may not be indicative of the true flow pattern during a particular time point given the relatively long data acquisition time. This is illustrated in Fig. 4, where high frame rate VFI is compared with full-view CFI frames that were acquired at the peak systole phase for three different stenosis percentages. As can be seen, the VFIs were able to provide a consistent visualization of the vortical flow beyond the stenotic point in the internal carotid artery (upper branch in the image). This kind of complex blood flow pattern may be of value to understanding the mechanism and progression of the stenosis. Although CFIs had a distinctly different appearance at the stenotic point (in the form of red-blue fast-changing color hues due to aliasing), their inaccurate flow estimates inherently make these images not suitable for deriving quantiative indicators of blood flow.

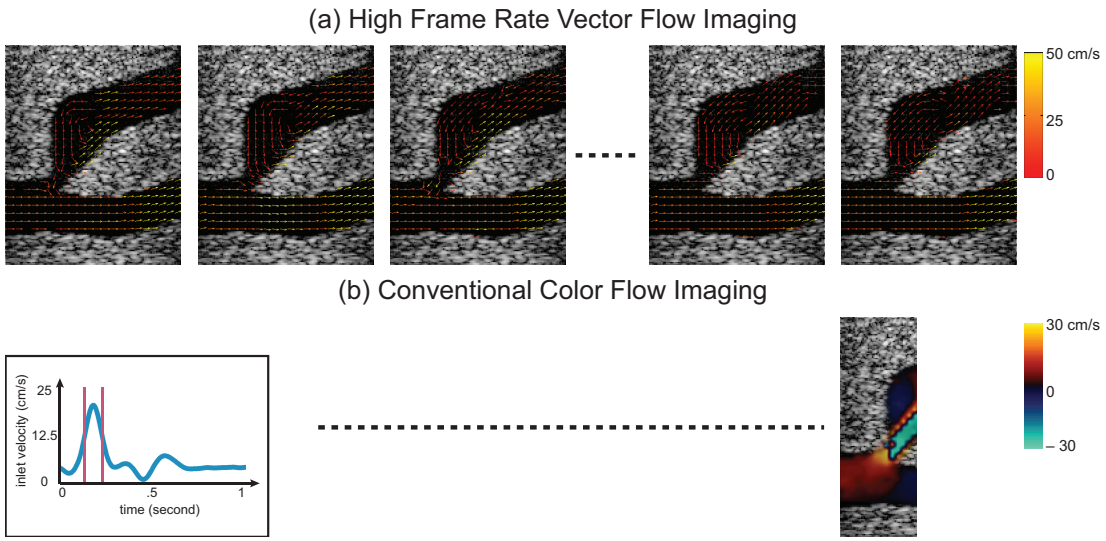

Fig. 3. Illustration of the achievable frame rate of (a) high frame rate VFI and (b) conventional CFI. The vertical lines shown on the inlet velocity graphs highlights the time period under investigation. With high frame rate VFI, 40 frames can be obtained while conventional CFI can only provides less than half of the image frame.

V. Discussion and Conclusion

In this work, high frame rate VFI has demonstrated its capabilities in overcoming the limitations of CFI as a carotid artery stenosis screening tool. In the future, we hope to extend upon this initial framework to obtain quantiative indicators of blood flow, such as turbulent index, vorticity and helicity. It is anticipated that these information can assist clinicians in making vascular disease diagnoses. They may also potentially shine new lights on the mechanism and progression of vascular diseases.

Acknowledgements

We would like to thank Prof. Paul Cheung and Prof K. W. Chow at HKU for their enthusiastic support and encouragement on this work.

References

[1] G. A. Donnan, M. Fisher, M. Macleod, and S. M. Davis, "Stroke," *Lancet*, vol. 371, pp. 1612–1623, 2008.

[2] European Carotid Surgery Trialists Collaborative Group, "Randomised trial of endarterectomy for recently symptomatic carotid stenosis: final results of the MRC European Carotid Surgery Trial (ECST)," *Lancet*, vol. 351, pp. 1379–1387, 1998.

[3] North American Symptomatic Carotid Endarterectomy Trial Collaborators, "Beneficial effect of carotid endarterectomy in symptomatic patients with high-grade carotid stenosis," *N. Engl. J. Med.*, vol. 325, pp. 445–453, 1991.

[4] U. S. Preventive Services Task Force, "Screening for carotid artery stenosis: U. S. Preventive Services Task Force recommendation statement," *Ann. Intern. Med.*, vol. 147, pp. 854–860, 2007.

[5] M. Tanter, J. Bercoff, L. Sandrin, and M. Fink, "Ultrafast compound imaging for 2-D motion vector estimation: application to transient elastography," *IEEE Trans. Ultrason. Ferroelec. Freq. Contr.*, vol. 49, no. 10, pp. 1363–1374, 2002.

[6] M. A. Lubinski, S. Y. Emelianov, and M. O'Donnell, "Speckle tracking methods for ultrasonic elasticity imaging using short-time correlation," *IEEE Trans. Ultrason. Ferroelec. Freq. Contr.*, vol. 46, pp. 82–96, 1999.

[7] J. A. Jensen and N. B. Svendsen, "Calculation of pressure fields from arbitrarily shaped, apodized, and excited ultrasound transducers," *IEEE Trans. Ultrason. Ferroelec. Freq. Contr.*, vol. 39, pp. 262–267, 1992.

[8] J. A. Jensen, "FIELD: A program for simulating ultrasound systems," *Med. Biol. Eng. Comput.*, vol. 34, pp. 351–353, 1996.

[9] R. F. Smith, B. K. Rutt, A. J. Fox, R. N. Rankin, and D. W. Holdsworth, "Geometric characterization of stenosed human carotid arteries," *Acad. Radiol.*, vol. 3, pp. 898–911, 1996.